

A Gain Scheduled Controller for Sinusoidal Ripple Elimination of AC PM Motor Systems

J. Wang, W. C. Gan and L. Qiu

Abstract— An adaptive control algorithm for the elimination of torque and velocity ripples in the Alternating Current (AC) Permanent Magnet (PM) motor control systems is presented in this paper. A model of AC PM motor system includes n sinusoidal disturbances is first developed. The internal model principle (IMP) is then applied to design a controller to eliminate the torque and velocity ripples without estimating the amplitude and the phase values of the sinusoidal disturbances. Based on the IMP and the pole-zero placement technique, a Gain Scheduled (GS) robust Two-Degree-of-Freedom (2DOF) speed regulator is developed to eliminate the torque and velocity ripples and to achieve a desirable tracking response. Using the small gain theorem, the system stability radius is obtained for n sinusoidal disturbances with slowly time-varying frequencies. The effectiveness of the proposed GS robust 2DOF speed regulator can be shown by the simulation results of an example with two sinusoidal disturbances.

I. INTRODUCTION

AC Permanent Magnet (PM) motors have been used in numerous industrial areas because of brushless and maintenance-free operation. For example, one of the typical applications can be found in the feed control of machine tools of the manufacturing industry, where accurate, smooth position and speed control are required [1], [2].

On the other hand, the main disadvantage of AC PM motors is torque ripples [3], [4]. Since AC PM motors aim at high performance applications such as machine tools or direct drive robotics, torque oscillations are not acceptable. Torque ripples lead to speed oscillations which deteriorate the system performance and limit the applications of AC PM motors in high-performance speed and position control systems.

There are many different techniques to eliminate the torque ripples of AC PM motor control systems. Broadly speaking, these techniques fall into two major categories. The first class consists of techniques that concentrate on the motor design so that it can eliminate the cogging and reluctance torque ripple generation of AC PM motors. Secondly, different adaptive control algorithms have been applied to eliminate the torque ripple of AC PM motor control systems [4].

In the past, the way to eliminate sinusoidal torque ripples in AC PM motor control systems is to purchase

high-grade components and the total cost of an automation machine is thus much increased [5]. To replace the inefficient and high-cost solution, we develop a novel and cost-effective speed control algorithm for torque ripple elimination in this paper.

In the present literature [5], the DC current offsets can be approximated by a sinusoidal function with a known frequency. The Internal Model Principle (IMP) and the pole-zero placement technique is then used to design a robust 2DOF speed regulator to eliminate the torque and velocity ripples with a single disturbance frequency. However, an AC PM motor control system usually has multiple output sinusoidal ripples. For example, DC offsets are always present at the motor terminals, gain error exists between phase; in addition, gain nonlinearity is difficult to avoid in the current control loop. The above disturbances can be modelled as sinusoidal functions with one, two and three times of the rotor electrical frequency respectively [6]. In this paper, the extension work of [5] is discussed and the proposed controller can be generalized to n sinusoidal disturbances. The stability radius of the system can also be derived with the small gain theorem. If the acceleration profile, is available to the controller, then the stability radius can be further enlarged.

This paper is organized as follows. In Section II, a brief review on the vector control of AC PM motors and the modeling of the torque ripples are given. In Section III, the IMP and the pole-zero placement technique is used to design a controller with the hypothesis that the disturbance frequencies are constants. Then the Gain Scheduled (GS) robust 2DOF speed regulator is developed for a time-varying disturbance frequencies in Section IV. The stability issue of the proposed GS robust 2DOF speed regulator is also addressed. With the acceleration profile input, the stability radius of the system is enlarged. The simulation results are presented in Section V to support the proposed controller. Finally, some concluding remarks are given in Section VI.

II. MODELING OF AC PM MOTORS AND DISTURBANCES

In this section, the vector control of AC PM motors is reviewed and the modeling of the torque ripples is described. In a practical high-performance AC PM motor control system, the basic components consist of a motion controller, a current tracking amplifier, a feedback encoder and an AC PM motor as shown in Fig. 1 [5].

This work is supported by Hong Kong Research Grants Council under Project HKUST6163/04E.

J. Wang was with the Department of Control Theory and Engineering, Harbin Institute of Technology, China.

W. C. Gan is with ASM Assembly Automation Ltd., Hong Kong.

L. Qiu is with the Department of Electrical and Electronic Engineering, The Hong Kong University of Science and Technology, Hong Kong, Hong Kong. eeqiu@ece.ust.hk

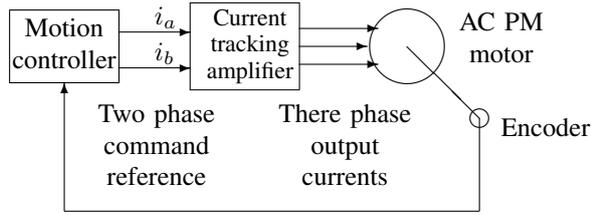


Fig. 1. An AC PM motor control system.

A. Modelling of AC PM Motors

A three phase AC PM motor current input model in the $d-q$ frame is given by the following equations [8],

$$\tau_e(t) = \frac{3P}{2} [\lambda_m i_q(t) - (L_q - L_d i_d(t) i_q(t))] \quad (1)$$

and

$$\tau_e(t) - \tau_l(t) = J_m \frac{d\omega(t)}{dt} + B_m \omega(t) \quad (2)$$

where the parameters and variables have the following meanings

P	number of poles (even number);
L_d, L_q	$d-q$ frame stator inductances;
J_m	moment of inertia;
B_m	friction constant;
λ_m	constant magnetic flux;
$i_d(t), i_q(t)$	$d-q$ frame stator currents;
$\tau_e(t)$	electro-mechanical torque;
$\tau_l(t)$	load torque;
$\omega(t)$	rotor mechanical speed;
$\omega_e(t) = \frac{P}{2}\omega(t)$	rotor electrical speed.

The vector control technique suggests to set $i_d(t) = 0$. This converts the nonlinear AC PM motor system into a linear system and the torque is linearly proportional to the input $i_q(t)$,

$$\tau_e(t) = \frac{3P}{2} \lambda_m i_q(t). \quad (3)$$

B. Modelling of the Sinusoidal Disturbances

The sinusoidal ripples are always present in the output of the AC PM motor [5]. Therefore, we can assume that there are n sinusoidal disturbances in the AC PM motor system and the frequencies of these n sinusoidal disturbances are already known and possibly slowly time-varying. In this case, the disturbance input, $d(t)$, is given by

$$d(t) = C + A_1 \sin(\omega_1(t)t + \phi_1) + A_2 \sin(\omega_2(t)t + \phi_2) + \dots + A_n \sin(\omega_n(t)t + \phi_n) \quad (4)$$

where C is an unknown constant, the disturbance frequency $\omega_i(t)$ ($i = 1, 2, \dots, n$) is a known time-varying function.

Our goal is to design a speed controller so that the output speed tracks a constant reference or a time-varying step reference and rejects the disturbances. The design objectives of the proposed controller are to have the controller order as low as possible, a good transient response,

and a fast disturbance rejection response even for the closed-loop system even when the system parameters are perturbed slightly.

III. ROBUST 2DOF REGULATOR DESIGN

Robust 2DOF regulators were discussed in [9]. In the following we assume that the disturbance and reference may have different modes. In reference to Fig. 2, the plant $G(s)$ is assumed to be a general single input single output (SISO) system while the reference input $r(t)$, and the disturbance input $d(t)$, are assumed to have possibly different modes.

Let $G(s)$ be a SISO plant described by a strictly proper transfer function $G(s) = b(s)/a(s)$, where

$$\begin{aligned} a(s) &= s^{n_a} + a_1 s^{n_a-1} + \dots + a_{n_a} \\ b(s) &= b_1 s^{n_a-1} + b_2 s^{n_a-2} + \dots + b_{n_a} \end{aligned}$$

and it is assumed that $a(s)$ and $b(s)$ are coprime. The general 2DOF controller shown in Fig. 2 can be written as

$$\begin{bmatrix} K_1(s) & -K_2(s) \end{bmatrix} = \frac{1}{k(s)} \begin{bmatrix} q(s) & -h(s) \end{bmatrix} \quad (5)$$

where

$$k(s) = s^{n_k} + k_1 s^{n_k-1} + \dots + k_{n_k} \quad (6)$$

$$q(s) = q_0 s^{n_k} + q_1 s^{n_k-1} + \dots + q_{n_k} \quad (7)$$

$$h(s) = h_0 s^{n_k} + h_1 s^{n_k-1} + \dots + h_{n_k}. \quad (8)$$

Then the 2DOF control structure becomes the following one as shown in Fig. 3. The transfer function from the input reference to the output is given by

$$\frac{Y(s)}{R(s)} = \frac{b(s)q(s)}{a(s)k(s) + b(s)h(s)} = \frac{b(s)q(s)}{\delta(s)}$$

and the transfer function from the disturbance input to the output is given by

$$\frac{Y(s)}{D(s)} = \frac{b(s)k(s)}{\delta(s)}$$

where $\delta(s)$ is the closed-loop characteristic polynomial of the system. Let the unstable modes of $r(t)$ be the roots of monic polynomial $m_r(s)$ and those of $d(t)$ be the roots of $m_d(s)$. Let the least common multiple of $m_r(s)$ and $m_d(s)$ be $m(s)$. It is well-known that the robust regulator problem is solvable, i.e., it is possible to design a controller so that the disturbance rejection and reference tracking are achieved, if and only if $m(s)$ and $b(s)$ are coprime. The detailed design of $q(s)$, $h(s)$ and $k(s)$ using IMP and pole placement technique can be found in [5].

IV. CONTROLLER DESIGN

In this section, the design of a Linear Time Invariant (LTI) robust 2DOF controller for a constant speed reference is first discussed. Then a GS robust 2DOF controller for a slowly time-varying speed step reference is designed by modifying the LTI controller.

The problem of accomplishing robust tracking and disturbance rejection is called the robust regulator problem.

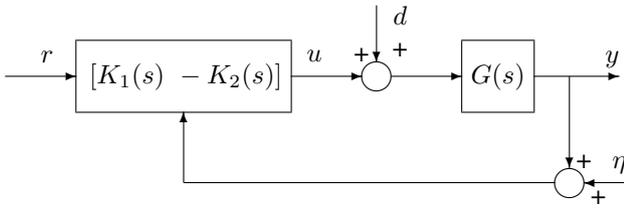


Fig. 2. A 2DOF controller structure.

The key idea is that the controller should include the unstable modes of the reference and disturbance according to the IMP. We also propose to use a 2DOF controller structure to achieve better transient responses and simpler designs. A 2DOF controller has a structure as shown in Fig. 2 with η denotes the sensor noise. One of its advantages, in comparison with the usual one degree of freedom or unity feedback structure, which amounts to setting $K_1(s) = K_2(s)$, is that the tracking performance depends mainly on $K_1(s)$, the robustness and the disturbance rejection performance depends only on $K_2(s)$. Hence $K_1(s)$ and $K_2(s)$ can be designed with different considerations [10].

A. Design of LTI 2DOF Controller with Constant Frequencies

The 2DOF regulator structure employed in our analysis is shown in Fig. 3. Here we follow the design procedure for the robust 2DOF regulator using pole-zero placement technique as in [5]. Since the reference $r(t)$ is a step reference, it follows that $m(s) = s$. The disturbance $d(t)$ contains n sinusoidal functions, it follows that

$$m_d(s) = s(s^2 + \omega_1^2)(s^2 + \omega_2^2) \cdots (s^2 + \omega_n^2).$$

Therefore

$$m(s) = s(s^2 + \omega_1^2)(s^2 + \omega_2^2) \cdots (s^2 + \omega_n^2).$$

It follows that $m(s)a(s)$ and $b(s)$ are coprime and a solution to the robust regulator problem based on the IMP exists. Since $n_a = 1$, we can choose $n_g = 0$. This leads to a controller of order equal to n_m , which is the lowest possible to achieve robust regulator. Hence

$$\begin{aligned} k(s) &= s(s^2 + \omega_1^2)(s^2 + \omega_2^2) \cdots (s^2 + \omega_n^2) \\ &= s^{2n+1} + k_1 s^{2n-1} + \cdots + k_n s, \end{aligned} \quad (9)$$

and $h(s)$, $q(s)$ have the following forms

$$\begin{aligned} h(s) &= h_0 s^{2n+1} + h_1 s^{2n} + \cdots + h_{2n+1} \\ q(s) &= q_0 s^{2n+1} + q_1 s^{2n} + \cdots + q_{2n+1}. \end{aligned}$$

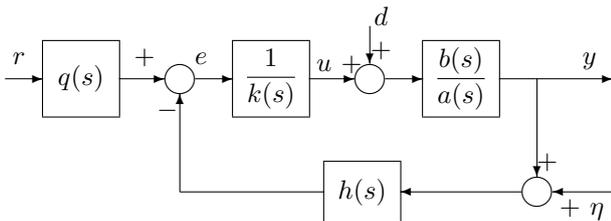


Fig. 3. A 2DOF regulator structure.

Choose the closed-loop poles $\alpha_1, \alpha_2, \dots, \alpha_{2n+1}$ according to the disturbance rejection specification and the remaining closed-loop poles α_{2n+2} according to the transient tracking response specification so that the closed-loop characteristic polynomial is

$$\begin{aligned} \delta(s) &= (s + \alpha_1)(s + \alpha_2) \cdots (s + \alpha_{2n+1}) \\ &= s^{2n+2} + \delta_1 s^{2n+1} + \delta_2 s^{2n} + \cdots + \delta_{2n+2}. \end{aligned}$$

Then by equating the coefficients of both sides of

$$\begin{aligned} \delta(s) &= k(s)a(s) + b(s)h(s) \\ &= s^{2n+2} + (a + bh_0)s^{2n+1} + (k_1 + bh_1)s^{2n} \\ &\quad + \cdots + (k_i + bh_{2i-1})s^{2n+2-2i} \\ &\quad + (ak_i + bh_{2i})s^{2n+1-2i} + \cdots + bh_{2n+1}, \end{aligned} \quad (10)$$

we can get

$$\begin{aligned} h_0 &= \frac{1}{b}(\delta_1 - a), & h_1 &= \frac{1}{b}(\delta_2 - k_1) \\ & & & \vdots \\ h_{2i} &= \frac{1}{b}(\delta_{2i+1} - ak_i), & h_{2i+1} &= \frac{1}{b}(\delta_{2i+2} - ak_{i+1}) \\ & & & \vdots \\ h_{2i} &= \frac{1}{b}(\delta_{2i+1} - ak_i), & h_{2n+1} &= \frac{1}{b}\delta_{2n+2}. \end{aligned} \quad (11)$$

Finally, as $m_r(s) = s$, we can arbitrarily assign the roots of $q(s)$. Here we choose the $2n + 1$ roots of $q(s)$ to be exactly the same as the roots of $\delta(s)$ subject to the constraint

$$\begin{aligned} q_{2n+1} &= h_{2n+1} \\ q(s) &= \frac{h_{2n+1}}{\prod_{i=1}^{2n+1} \alpha_i} (s + \alpha_1) \cdots (s + \alpha_{2n+1}). \end{aligned} \quad (12)$$

The coefficients of $q(s)$, q_i ($i = 1, 2, \dots, n$) are obtained. The transfer function is finally given by

$$\frac{Y(s)}{R(s)} = \frac{\alpha_{2n+2}}{s + \alpha_{2n+2}}.$$

B. Slowly Time-Varying Frequencies

When the sinusoidal disturbances have time-varying frequencies, we need to include internal modes which vary with the disturbance frequencies; other parameters of the controller in general also need to be changed with time to ensure that the closed-loop system is stable. The disturbance frequencies ω_i and controller coefficients k_i in (9), (10) and (11) are replaced by $\omega_i(t)$ and $k_i(t)$ ($i = 1, 2, \dots, n$) respectively. Using the following observer

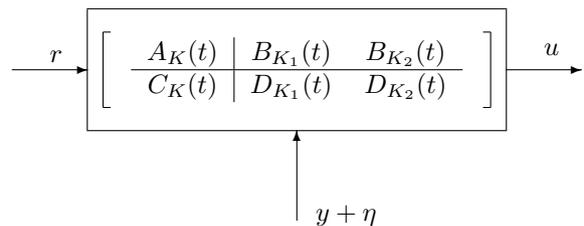


Fig. 4. The GS robust 2DOF speed regulator.

canonical realization to implement the regulator with

$$\hat{x}(t) = [x_1(t) \quad x_2(t) \quad \cdots \quad x_{2n+1}(t)]'$$

and

$$v(t) = [r(t) \quad y(t) + \eta(t)]',$$

we get

$$\begin{aligned} \dot{\hat{x}}(t) &= A_K(t)\hat{x}(t) + [B_{K_1} \quad B_{K_2}]v(t) \\ u(t) &= C_K(t)\hat{x}(t) + [D_{K_1} \quad D_{K_2}]v(t) \end{aligned}$$

where

$$\begin{aligned} A_K(t) &= \begin{pmatrix} N_{2n \times 1}(t) & I_{2n \times 2n} \\ 0 & 0_{1 \times 2n} \end{pmatrix} \\ B_K(t) &= \begin{pmatrix} q_1 & -h_1(t) \\ q_2 - q_0 n_1(t) & -h_2(t) + h_0(t)k_1(t) \\ q_3 & -h_3(t) \\ \vdots & \vdots \\ q_{2i} - q_0 n_i(t) & -h_{2i}(t) + h_0(t)k_i(t) \\ q_{2i+1} & -h_{2i+1}(t) \\ \vdots & \vdots \\ q_{2n+1} & -h_{2n+1}(t) \end{pmatrix} \\ C_K(t) &= [1 \quad 0 \quad \cdots \quad 0 \quad 0]_{1 \times (2n+1)} \\ D_K(t) &= [q_0 \quad -h_0(t)] \end{aligned}$$

and

$$N_{2n \times 1}(t) = [0 \quad k_1(t) \quad 0 \quad k_2(t) \quad \cdots \quad 0 \quad k_n(t)]'$$

Fig. 4 shows the block diagram of the GS robust 2DOF speed regulator and the linearized AC PM motor system plant can be represented by the following state space equations [11]

$$\begin{aligned} \dot{x}_{2n+2}(t) &= -ax_{2n+2}(t) + b[u(t) + d(t)] \\ y(t) &= x_{2n+2}(t). \end{aligned}$$

Let

$$\begin{aligned} \tilde{x}(t) &= [x_1(t) \quad x_2(t) \quad \cdots \quad x_{2n+2}(t)]' \\ w(t) &= [r(t) \quad d(t) \quad \eta(t)]' \\ \tilde{y}(t) &= [u(t) \quad y(t)]' \end{aligned}$$

the closed-loop state space equations can be written as follows

$$\begin{aligned} \dot{\tilde{x}}(t) &= A(t)\tilde{x}(t) + B(t)w(t) \\ \tilde{y}(t) &= C(t)\tilde{x}(t) + D(t)w(t). \end{aligned}$$

The problem now boils down to choose the transformation matrix $P(t)$ to transform $A(t)$ into an observer canonical form so as to facilitate the stability analysis by the small gain theorem. Let

$$z(t) = [z_1(t) \quad z_2(t) \quad \cdots \quad z_{2n+2}(t)]'$$

be the new state variables. We have

$$\tilde{x}(t) = P(t)z(t)$$

and

$$P(t) = \begin{pmatrix} 0 & 0 & 1 & 0 & \cdots & 0 & 0 \\ 0 & 0 & 0 & 0 & \cdots & 0 & -k_n(t) \\ \vdots & \vdots & \vdots & \vdots & \cdots & \vdots & \vdots \\ \vdots & \vdots & \vdots & \vdots & \cdots & \vdots & 0 \\ \vdots & \vdots & \vdots & \vdots & \cdots & \vdots & -k_i(t) \\ \vdots & \vdots & \vdots & \vdots & \cdots & \vdots & \vdots \\ 0 & 0 & 0 & 0 & \cdots & 0 & -k_1(t) \\ 1 & 0 & 0 & 0 & \cdots & 0 & 0 \\ 0 & 0 & 0 & 0 & \cdots & 0 & b \end{pmatrix}$$

The closed-loop system state space equations can be transformed into the following

$$\begin{aligned} \dot{z}(t) &= A_z(t)z(t) + B_z(t)\tilde{u}(t) \\ \tilde{y}(t) &= C_z(t)z(t) + D_z(t)\tilde{u}(t) \end{aligned}$$

where

$$A_z(t) = \begin{pmatrix} 0 & 0 & 1 & \cdots & -\delta_{2n+2} \\ 1 & 0 & 0 & \cdots & -\delta_{2n+1} - k_1(t) \\ \vdots & \vdots & \vdots & \cdots & \vdots \\ \vdots & \vdots & \vdots & \cdots & -\delta_{2i} \\ \vdots & \vdots & \vdots & \cdots & -\delta_{2n+1-2i} - k_i(t) \\ \vdots & \vdots & \vdots & \cdots & \vdots \\ 0 & 0 & 0 & \cdots & -\delta_1 \end{pmatrix}$$

$$\begin{aligned} B_z(t) &= \begin{pmatrix} q_{2n+1} & 0 & -h_{2n+1}(t) \\ q_{2n} & n_n(t) & -h_{2n}(t) \\ q_{2n-1} & 0 & -h_{2n-1}(t) \\ q_{2n-2} & n_{n-1}(t) & -h_{2n-2}(t) \\ \vdots & \vdots & \vdots \\ q_{2i} & n_{n-i+1}(t) & -h_{2i}(t) \\ q_{2i-1} & 0 & -h_{2i-1}(t) \\ \vdots & \vdots & \vdots \\ bq_0 & b & -bh_0(t) \end{pmatrix} \\ C_z(t) &= \begin{pmatrix} 0 & 0 & 1 & 0 & \cdots & 0 & -bh_0(t) \\ 0 & 0 & 0 & 0 & \cdots & 0 & b \end{pmatrix} \\ D_z(t) &= \begin{pmatrix} q_0 & 0 & -h_0(t) \\ 0 & 0 & 0 \end{pmatrix} \end{aligned}$$

Here $A_z(t)$ is a $(2n+2) \times (2n+2)$ matrix. Suppose I_{kj} is the entry of the the first $2n+1$ columns in A_z , where

$$I_{kj} = \begin{cases} 1 & k = 2i, j = 2n - 2i + 2 \\ & k = 2i - 1, j = 2i + 1 \quad (i = 1, 2 \cdots n) \\ 0 & \text{otherwise} \end{cases}$$

and $B_z(t) \in \mathbb{R}^{(2n+2) \times 3}$ and $C_z(t) \in \mathbb{R}^{2 \times (2n+2)}$. Next let

$$\begin{aligned} L(t) &= P^{-1}(t)\dot{P}(t) \\ &= [0 \quad -\dot{k}_1(t) \quad 0 \quad \cdots \quad -\dot{k}_n(t) \quad 0 \quad 0]' \end{aligned}$$

and

$$M = P^{-1}(t)A_z(t)P(t).$$

Therefore,

$$M = \begin{pmatrix} 0 & 0 & 1 & \cdots & -\delta_{2n+2} \\ 1 & 0 & 0 & \cdots & -\delta_{2n+1} \\ \vdots & \vdots & \vdots & \cdots & \vdots \\ \vdots & \vdots & \vdots & \cdots & -\delta_{2i} \\ \vdots & \vdots & \vdots & \cdots & -\delta \\ \vdots & \vdots & \vdots & \cdots & \vdots \\ 0 & 0 & 0 & \cdots & -\delta_1 \end{pmatrix}.$$

Here M is a $(2n+2) \times (2n+2)$ matrix.

According to the small gain theorem [11], the associated autonomous system

$$\begin{aligned} \dot{z}(t) &= A_z(t)z(t) \\ &= \left(M + RL(t) \begin{bmatrix} 0 & \cdots & 0 & 1 \end{bmatrix}_{1 \times (2n+2)} \right) z(t) \end{aligned}$$

is internally uniformly exponentially stable if the following condition is satisfied:

$$\begin{aligned} \|L(t)\|_\infty &< \left\| \begin{bmatrix} 0 & \cdots & 0 & 1 \end{bmatrix}_{1 \times (2n+2)} (sI - M)^{-1} R \right\|_\infty^{-1} \\ &= \left\| \frac{\begin{bmatrix} 0 & s & \cdots & 0 & s^{2i-1} & \cdots & s^{2n-1} & 0 & 0 \end{bmatrix}}{\delta(s)} \right\|_\infty^{-1} \\ &= r_s \end{aligned} \quad (13)$$

where R is a $(2n+2) \times (2n+2)$ matrix. In the $2i$ th row, the $2i$ th column is 1, the other entries are zeros and r_s is defined as the stability radius. The internal stability of the closed-loop system is preserved as long as $\|L(t)\|_\infty$ is less than r_s in (13). Since the matrices $B_z(t)$, $C_z(t)$ and $D_z(t)$ associated with the closed-loop system are bounded, it follows from, the closed-loop system is also bounded-input bounded-output stable if (13) is satisfied. If the acceleration profile, is available to the controller, then the stability radius can be further enlarged by modifying the feedback gains $h_{2i}(t)$ as

$$h_{2i}(t) = \frac{1}{b} (\delta_{2i+1} - ak_i(t) - \dot{k}_i(t)).$$

V. SIMULATION RESULTS

TABLE I
MOTOR PARAMETERS

J_m	$0.144 \times 10^{-4} \text{kg} \cdot \text{m}^2$
B_m	$5.416 \times 10^{-4} \text{Nm/rad} \cdot \text{s}^{-1}$
λ_m	0.0283Wb
P	8
$K_t = \frac{3}{2} \frac{P}{\lambda_m}$	0.1698Nm/A

A 50 W AC PM motor is used in our simulations tests and the motor parameters are listed in TABLE I. The gain difference between motor driver phases and the offset currents are always present in the AC PM motor system, so the torque ripples can be modelled as two sinusoidal functions whose frequencies depend on the motor speed,

$$\tau_{\text{off}}(t) = A_{d1} \sin(\omega_1(t)t - \phi_1) + A_{d2} \sin(\omega_2(t)t - \phi_2)$$

where $\omega_1(t) = \omega_e(t) \approx \frac{P}{2} \omega_r(t)$ and $\omega_2(t) = \frac{1}{2} \omega_e(t) \approx \frac{P}{4} \omega_r(t)$ are defined as the disturbance frequencies respectively.

According to the design procedure listed in Section IV, one of the possible solutions is to choose the six closed-loop poles at 140, 150, 160, 170, 180 and 190, and the five closed-loop zeros at 150, 160, 170, 180, and 190 respectively. Other choices of the pole and zero locations are possible but too fast closed-loop poles may lead to the signal saturation problem and the current loop dynamics may not be neglected if the bandwidth of the speed loop is close to that of the current loops. The GS robust 2DOF speed regulator is designed to satisfy the motion specifications with zero overshoot and rise time less than 60 ms.

The stability of this GS robust 2DOF speed regulator depends on the stability radius r_s . Let

$$\psi(t) = \begin{bmatrix} 0 & -(\omega_1^2(t) + \omega_2^2(t))' & 0 & -(\omega_1^2(t)\omega_2^2(t))' & 0 & 0 \end{bmatrix},$$

according to the small gain theorem, the closed loop stability is ensured if

$$\begin{aligned} \|\psi\|_\infty &= \sup_{t \geq 0} \|\psi(t)\|_2 \\ &< \left\| \frac{\begin{bmatrix} 0 & s & 0 & s^3 & 0 & 0 \end{bmatrix}}{s^6 + \delta_1 s^5 + \delta_2 s^4 + \delta_3 s^3 + \delta_4 s^2 + \delta_5 s + \delta_6} \right\|_\infty^{-1} \\ &= r_s. \end{aligned}$$

For the simulations, two profiles satisfying $\|\psi\|_\infty < r_s$ and $\|\psi\|_\infty > r_s$ respectively are employed to test the proposed GS robust 2DOF speed regulator.

In order to demonstrate the effectiveness of the use of the IMP, another robust 2DOF regulator is designed without including the sinusoidal disturbance modes to track the first input profile. This can be done by simply assigning $k(s) = s$ and the dominant closed-loop pole of this robust 2DOF regulator is placed at -140 , the same one of the GS robust 2DOF speed regulator. Fig. 5 shows the speed output is contaminated with ripples by the two sinusoidal disturbances. On the other hand, with the help of the sinusoidal modes inside the speed regulator, the output speed response of the GS robust 2DOF speed regulator achieves a desirable tracking response without any velocity ripple contamination as shown in the Fig. 6.

For the second input profile, we first test it without the acceleration profile input. The speed response is shown

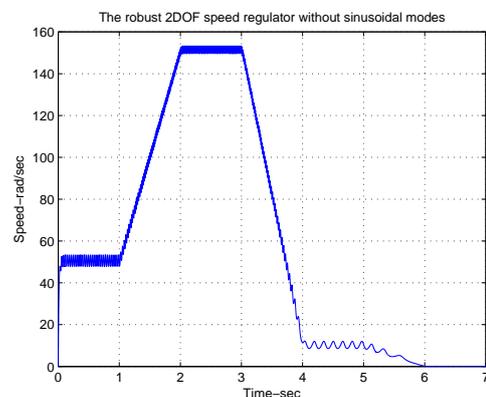


Fig. 5. Speed output with a general 2DOF regulator.

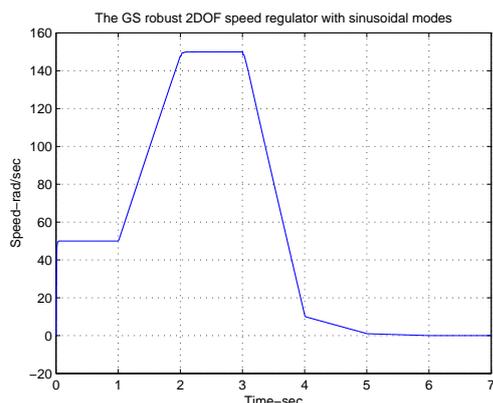


Fig. 6. Speed output with the GS robust 2DOF regulator.

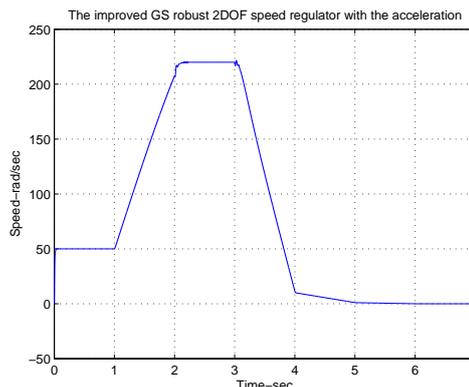


Fig. 8. Speed output with the acceleration profile input.

in Fig. 7 and the output speed response is not good in general and at $t = 3s$ as the value of $\|\psi\|_{\infty}$ exceeds r_s , the output speed becomes unstable and oscillatory. However, if the improved GS robust 2DOF speed regulator is implemented with the acceleration profile input, a comparatively good speed response is obtained and shown in Fig. 8, and the stability of the whole system remains. Smooth transitions can still be maintained during the high speed reference change at $t = 2s$ and $t = 3s$. This simulation result shows the stability radius of the overall system can be enlarged with the availability of the acceleration input profile.

VI. CONCLUSIONS

In summary, the GS robust 2DOF regulators based on the IMP and the pole-zero placement algorithm can eliminate the ripples due to sinusoidal disturbances, as long as the disturbance frequencies do not change too fast. When the condition in (13) is satisfied, implementing with $\dot{k}_i(t)$ in $h_{2i}(t)$, an infinity stability radius can be achieved. The proposed controller is not limited to the application of AC PM motor systems, but can be applied to any servo problems with n sinusoidal disturbances with known frequencies.

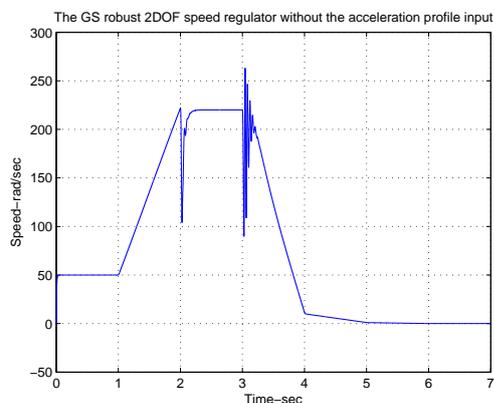


Fig. 7. Speed output without the acceleration profile input.

REFERENCES

- [1] D. Chen and B. Paden, "An adaptive linearization of hybrid step motors: Stability analysis," *IEEE Trans. on Automatic Control*, vol. 38, no. 6, pp. 874–887, Jun. 1993.
- [2] Y. Liu and D. Chen, "Adaptive rejection of velocity-ripple from position transducer in a motion control system," *Proc. 33rd IEEE Conf. Decision and Control*, vol. 1, pp. 690–695, Dec. 1994.
- [3] V. Petrovic, R. Ortega, A. M. Stankovics, and G. Tadmor, "Design and implementation of an adaptive controller for torque ripple minimization in PM synchronous motors," *IEEE Trans. on Power Electronics*, vol. 15, pp. 871–880, Sep. 2000.
- [4] G. Ferretti, G. Magnani and P. Rocco, "Modeling, identification, and compensation of pulsating torque in permanent magnet AC motors," *IEEE Trans. on industrial Electronics*, vol. 45, pp. 912–920, Dec. 1998.
- [5] W. C. Gan and L. Qiu, "Torque velocity ripple elimination of AC permanent magnet motor control systems using the internal model principle," *IEEE/ASME Trans. on Mechatronics*, vol. 9, pp. 436–447, Jun. 2004.
- [6] W. C. Gan, S. W. Tam, K. K. C. Chen and G. P. Widdowson, "Analysis of motor driver uncertainties in linear permanent magnet motor control systems," *Proc. of The Fifth International Symposium on Linear Drives for Industry Applications, LDIA'05*, Sep. 2005.
- [7] P. Pillay and R. Krishnan, "Modeling of permanent magnet motor drives," *IEEE Trans. on Industry Electronics*, vol. 13, pp. 388–400, Nov. 1998.
- [8] D. W. Novotny and T. A. Lipo, *Vector Control and Dynamics of AC Drives*, New York: Oxford, 1998.
- [9] W. A. Wolovich, *Automatic Control Systems*, FortWorth, TX: Sauders College Publishing, 1994.
- [10] K. Zhou and R. Zhang, "A new controller architecture for high performance, robust, and fault tolerant control," *IEEE Trans. on Automatic Control*, vol. 40, no. 10, pp. 4120–4125, Oct. 2000.
- [11] M. Vidyasagar, *Control System Synthesis*, Cambridge, MA: MIT Press, 1985.